Pacific Northwest
NATIONAL LABORATORY

PNNL-33519

First-Principles Study of Tritium Trapping by Point Defects in Fe-Al Aluminide Coating Phases

September 2022

Michel Sassi
Anne M. Chaka
David J. Senor
Andrew M. Casella

U.S. DEPARTMENT OF ENERGY | Prepared for the U.S. Department of Energy under Contract DE-AC05-76RL01830

DISCLAIMER

PACIFIC NORTHWEST NATIONAL LABORATORY
operated by
BATTELLE
for the
UNITED STATES DEPARTMENT OF ENERGY
under Contract DE-AC05-76RL01830

Printed in the United States of America

Available to DOE and DOE contractors from the
Office of Scientific and Technical Information,
P.O. Box 62, Oak Ridge, TN 37831-0062;
ph: (865) 576-8401
fax: (865) 576-5728
email: reports@adonis.osti.gov

Available to the public from the National Technical Information Service
5301 Shawnee Rd., Alexandria, VA 22312
ph: (800) 553-NTIS (6847)
email: orders@ntis.gov <https://www.ntis.gov/about>
Online ordering: http://www.ntis.gov

PNNL-33519

First-Principles Study of Tritium Trapping by Point Defects in Fe-Al Aluminide Coating Phases

September 2022

Michel Sassi
Anne M. Chaka
David J. Senor
Andrew M. Casella

Prepared for
the U.S. Department of Energy
under Contract DE-AC05-76RL01830

Pacific Northwest National Laboratory
Richland, Washington 99354

Summary

Density functional theory simulations have been carried out to investigate the potential for tritium trapping by metal vacancies in five different Fe-Al aluminide coating phases. It was found that tritiation of Fe and Ni vacancies is generally less favorable than the tritiation of Al vacancies. However, for the first tritiation, a trend in the defect formation energy can be obtained such that metal defects in the Fe_2Al_x family of materials (i.e., Fe_2Al_4, Fe_2Al_5, and Fe_2Al_6) trap tritium species more favorably than metal vacancies in Fe_4Al_{13} and $FeNiAl_5$. Further investigations using *ab initio* thermodynamics calculations confirmed that trend for a range of tritium partial pressure at a temperature of 700 K. Especially, it was shown that the energy difference between tritiated and non-tritiated metal vacancies is smaller and more favorable for the Fe_2Al_x family, followed by Fe_4Al_{13}, and $FeNiAl_5$. While this study shows that tritium interacts differently in the various Fe-Al aluminide phases, it also suggests that tritium trapping and retention could be more efficient if metal defects are present in some Fe-Al phases.

1.0 Introduction

In the design of the TPBAR the inner surface of the 316SS structural pressure boundary cladding is coated with an iron aluminide (Fe-Al) matrix to reduce tritium permeation into the surrounding coolant. Although the vast majority of tritium is absorbed by the getter, post-irradiation evaluation (PIE) indicates that a small fraction of tritium is trapped in the aluminide coating.[1] The mechanism of how this trapping occurs and how it may be prevented is not known. The purpose of the investigation described in this report is to assess the relative energy of interstitial and substitutional tritium (e.g., T_{Fe} or T_{Al} sites) in Fe-Al phases, and to evaluate the potential for point defects to trap tritium in various Fe-Al bulk phases constituting the aluminide coating of TPBAR using *ab initio* calculations based on density functional theory (DFT). The interstitial binding energies were also compared between each Fe-Al phase for in-reactor conditions.

The structure and composition of major phases in the outer aluminide layer for Cycle 13 before and after irradiation have been determined by Edwards and coworkers[2] using scanning transmission electron microscopy (STEM). Image analysis and chemical mapping revealed the presence of three bulk phases in the outer layer of the unirradiated coating, as shown in Figure 1. Those phases were identified as $NiFeAl_5$ (hexagonal), Fe_4Al_{13} (monoclinic), and Fe_2Al_5 (orthorhombic), and it was found that neutron irradiation didn't appear to alter these bulk phases. Previous work on the Fe_2Al_5 phase[3] has identified a structural peculiarity consisting of Al-filled channels parallel to the *c*-axis, shown as yellow spheres in the atomistic structure at the right in Figure 1, giving rise to an approximate composition of Fe_2Al_5. Previous *ab initio* modelling[3,4] of bulk Fe_2Al_5 suggested that at high temperature (1300 K) the channel of Al atoms diffused in a liquid-like manner along the *c*-axis due to the presence of Al vacancies (V_{Al}) in the structure. Therefore, three stoichiometries for Fe_2Al_x phases, namely Fe_2Al_4, Fe_2Al_5, and Fe_2Al_6, were studied to evaluate the impact of Al vacancy concentration on tritium trapping. Atomistic and DFT optimized models of these three stoichiometries of Fe_2Al_x phases (x=4, 5, 6), as well as the $FeNiAl_5$ and Fe_4Al_{13} phases were previously developed for the FY21 diffusion study by Sassi *et al.*[5] in which it was found that interstitial tritium would diffuse faster in Fe_2Al_x phases, followed by Fe_4Al_{13}, then $FeNiAl_5$, as shown by the diffusion coefficients calculated at a temperature of 600 K in Figure 1.

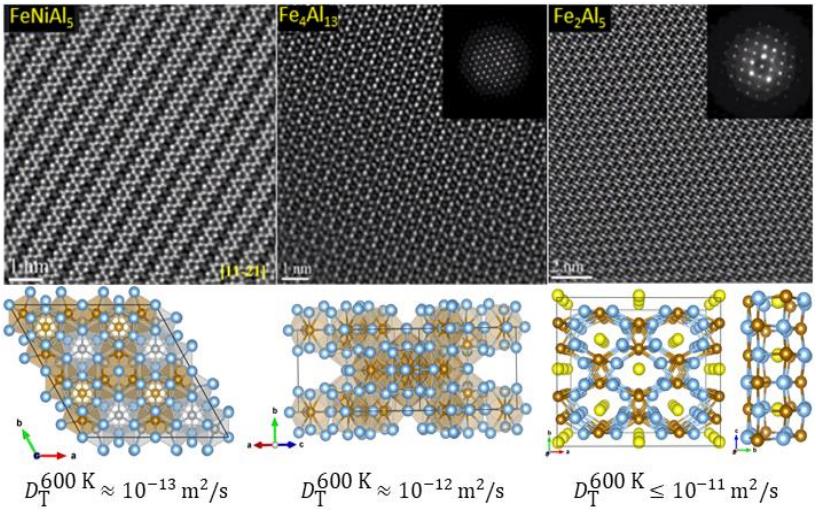

Figure 1: STEM atomic column imaging of three ($FeNiAl_5$, Fe_4Al_{13}, and Fe_2Al_5) bulk phases in unirradiated coating (courtesy of D. Edwards FY20[2]), their atomistic representation, and calculated tritium diffusion coefficient at 600 K.[5]

2.0 Computational Details

Density functional theory calculations have been performed with the VASP code.[6] All the simulations used the generalized gradient approximation (GGA) exchange-correlation as parametrized in the Perdew, Burke, and Ernzerhof (PBE) functional.[7] A cutoff energy of 350 eV for the plane-wave basis set has been used and spin-polarization has been taken into account.

The lattice parameters and atomic coordinates of defect-free supercells of $FeNiAl_5$,[8] Fe_4Al_{13},[9] and three Fe_2A_x phases,[3,10] namely Fe_2Al_4, Fe_2Al_5, and Fe_2Al_6, were fully relaxed using a convergence criterion of 10^{-5} eV/cell for the total energy and 10^{-4} eV/Å for the force components. Table 1 summarizes the supercell sizes and Monkhorst-Pack[11] *k*-point mesh used to sample the Brillouin zone in each case.

Fe-Al phase	Supercell size	*k*-point mesh
$FeNiAl_5$	2×2×2 (224 atoms)	2×2×2
Fe_4Al_{13}	1×1×1 (102 atoms)	2×4×3
Fe_2Al_4	2×2×3 (144 atoms)	2×2×2
Fe_2Al_5	2×2×3 (168 atoms)	2×2×2
Fe_2Al_6	2×2×3 (192 atoms)	2×2×2

Table 1: Summary of the supercell sizes and Monkhorst-Pack *k*-point mesh sampling used in this study.

Starting from the optimized defect-free crystal structures, a single metal vacancy was introduced. In these simulations, only the atomic coordinates were allowed to relax while the lattice parameters were kept fixed to their relaxed defect-free bulk structure values. Subsequently, tritium loading of the metal vacancy has been investigated by filling it with several tritium atoms. Multiple configurations were calculated and only the most energetically favorable ones are reported. Due to their similar electronic structure, the pseudopotential of standard hydrogen (^{1}H) has been used to describe tritium (^{3}H), however, to account for the isotopic effect, the mass in the pseudopotential has been modified to match that of the isotope atom.

To evaluate the relative stability of non-tritiated and tritiated metal vacancies at conditions relevant to in-reactor operation, *ab initio* thermodynamics calculations have been carried out in which the temperature (T) and tritium partial pressure ($p(\mathrm{T_2})$) dependance of the Gibbs free energy of formation of defects, $\Delta G_f(T, p(\mathrm{T_2}))$, has been calculated using the following equation:

$$\Delta G_f(T, p(\mathrm{T_2})) = \left(E^T_{\text{defect}} + E^{ZPE}_{\text{defect}} + \Delta\mu(T)_{\text{defect}}\right) - \left(E^T_{\text{perf}} + E^{ZPE}_{\text{perf}} + \Delta\mu(T)_{\text{perf}}\right) + \sum_i n_i(E^T_i + E^{ZPE}_i + \Delta\mu_i(T, p(\mathrm{T_2}))) \quad (1)$$

n_i is the number of atoms added/removed of each atomic species i. E^T_i, E^{ZPE}_i, and $\Delta\mu_i(T, p(\mathrm{T_2}))$ are respectively the total DFT energy, the zero-point-energy, and the temperature and T_2 partial pressure dependent chemical potential of each reference species i. In order to account for temperature effect in the various Fe-Al bulk phases, $\Delta\mu(T)_{\text{defect}}$ and $\Delta\mu(T)_{\text{perf}}$ are the temperature-dependent chemical potential of the system with and without defect (i.e., perfect). All the temperature-dependent chemical potentials have been calculated using the following relation:

$$\Delta\mu(T) = (H(T) - H^{\circ}(298.15)) - TS \quad (2)$$

where $H(T)$ and $H^{\circ}(298.15)$ are the system enthalpy at a temperature T and at T=298.15 K, and S is the entropy. Here, $H(T)$, is the Helmholtz free energy as given by $H(T) = -k_B T \ln(Z)$, where Z is the partition function expressed as implemented in the Phonopy code.[12] The calculated

temperature dependence of chemical potential of tritium is shown in Figure 2. While there are no available experimental data for tritium, the trends between calculated and experimental data[13] available for H_2 and D_2 are in good agreement, which give confidence in the calculated chemical potential for T_2. The temperature and T_2 partial pressure dependent chemical potential of molecular T_2 has been calculated as:

$$\Delta\mu_{T_2}(T, p(T_2)) = \mu_{T_2}\left(T^{\circ}, p^{\circ}(T_2)\right) + k_B T \log\left(\frac{p(T_2)}{p^{\circ}(T_2)}\right) \quad (3)$$

where T° and $p^{\circ}(T_2)$ are the temperature and T_2 partial pressure at standard conditions.

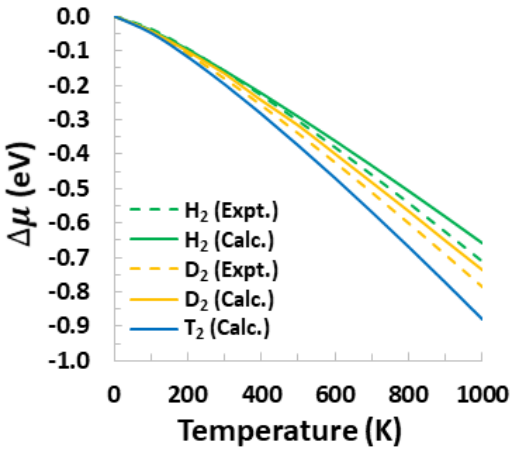

Figure 2: Temperature-dependence of the chemical potential of hydrogen isotopes.

3.0 Results and Discussion

3.1 Tritiation of metal vacancies in $FeNiAl_5$

Based on the hexagonal symmetry of $FeNiAl_5$, a single metal vacancy (V_M) was created at different atomic sites to identify those most favorable for vacancy formation. As shown in Table 2, there is a range of vacancy formation energies for the same element as the surrounding coordination geometry and near neighbors can vary within a phase. In $FeNiAl_5$, for example, the generation of a Fe, Ni, or Al vacancy can respectively be less energetically favorable by 0.74 eV, 0.61 eV, or 0.58 eV compared to the lowest energy sites depending upon position. Along with a structural representation of $FeNiAl_5$, a single polyhedron is shown in Figure 3a for each species to help identify the position of the most favorable sites for vacancy formation.

Phase	Defect type	Energy variations (eV)
$FeNiAl_5$	V_{Fe} (4)	$0 \leq E_v \leq 0.74$
	V_{Ni} (4)	$0 \leq E_v \leq 0.61$
	V_{Al} (6)	$0 \leq E_v \leq 0.58$
Fe_4Al_{13}	V_{Fe} (6)	$0 \leq E_v \leq 0.38$
	V_{Al} (21)	$0 \leq E_v \leq 1.37$
Fe_2Al_4	V_{Fe} (4)	$0 \leq E_v \leq 0.03$
	V_{Al} (6)	$0 \leq E_v \leq 0.02$
Fe_2Al_5	V_{Fe} (4)	$0 \leq E_v \leq 0.03$
	V_{Al} Channel (1)	-
	V_{Al} (6)	$0 \leq E_v \leq 0.05$
Fe_2Al_6	V_{Fe} (4)	$0 \leq E_v \leq 0.02$
	V_{Al} Channel (1)	-
	V_{Al} (6)	$0 \leq E_v \leq 0.03$

Table 2: Summary of the relative energy variations for the creation a metal vacancy in the different FeAl phases investigated. The number between brackets indicates the number of atomic sites explored for vacancy generation.

Investigations of the effect of tritium loading in metal vacancies were performed for the lowest energy defect identified. As shown in Figure 3b, the tritiation of Fe and Ni vacancies is found to be less energetically favorable than non-tritiated defects. The insertion of one tritium atom increases the defect energy by 0.69 eV and 0.48 eV for the Fe and Ni vacancy respectively, suggesting that the formation of Al—T bonds are not energetically favorable. In the case of an Al vacancy, the insertion of one tritium atom is found to lower the energy cost of forming the vacancy by 0.13 eV due to the formation of a Fe—T bond.

To evaluate the potential for tritium trapping by a metal vacancy, the trapping energy, E_{Trap}, defined as $E_{\text{Trap}} = E_{\text{V}_\text{M}^\text{T}} - E_{(\text{V}_\text{M}+1\text{T}_i)}$ has been calculated, in which $E_{(\text{V}_\text{M}+1\text{T}_i)}$ is the combined energetic cost of an interstitial tritium (T_i) and a metal vacancy (V_M), and $E_{\text{V}_\text{M}^\text{T}}$ is the energy cost of a singly tritiated metal vacancy. While the value of $E_{(\text{V}_\text{M}+1\text{T}_i)}$ is reported in Figure 3b by short line symbols, the value of E_{Trap} is 0.41 eV, 0.20 eV, and -0.42 eV for the Fe, Ni, and Al species respectively.

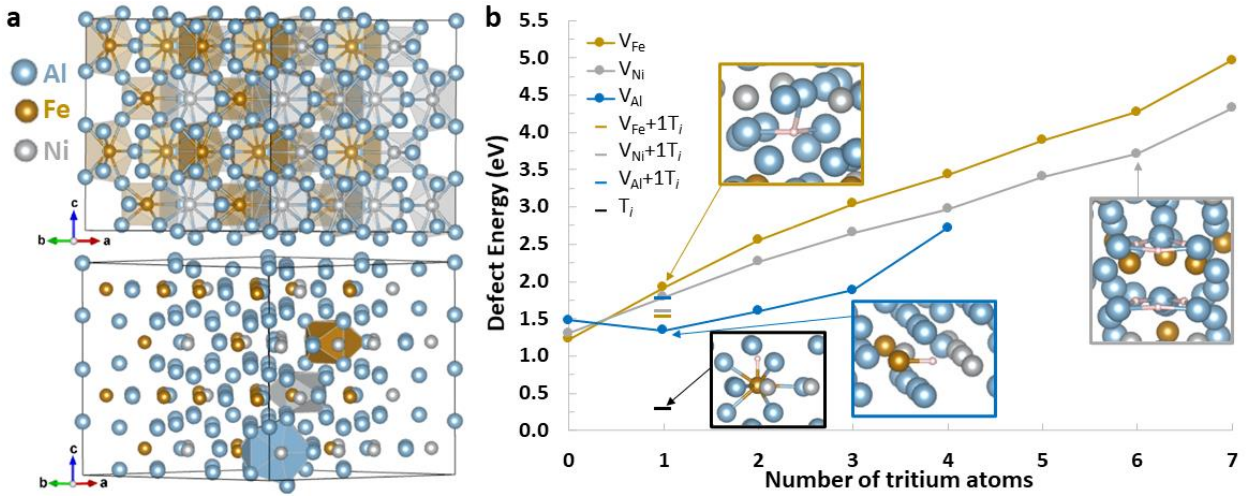

Figure 3: (a) Structural representation of the hexagonal $FeNiAl_5$ phase along with the location of the lowest energy vacancy defects for Fe, Ni, and Al species as highlighted by a polyhedron. (b) Defect formation energy of metal vacancies as function of tritium loading.

3.2 Tritiation of metal vacancies in Fe_4Al_{13}

To investigate metal defects in the monoclinic Fe_4Al_{13} phase, single vacancies have been generated at 6 and 21 different Fe and Al sites respectively. As shown in Table 2, while an energy difference of 0.38 eV between the most and least favorable vacancy site has been obtained for Fe, a much larger energy variation is obtained for Al sites for which the least favorable vacancy cost up to 1.37 eV more than the most favorable Al vacancy site. The location of the most favorable Fe and Al sites for a vacancy have been highlighted in Figure 4a by a polyhedron.

The impact of tritium loading on the formation energy of Fe and Al vacancies is shown in Figure 4b. Similarly to $FeNiAl_5$, the tritiation of Fe vacancy in Fe_4Al_{13} is generally found to increase the energy cost of a vacancy, whereas the tritiation of an Al vacancy tends to reduce the overall energy cost for up to three tritium atoms. In the case of an Al vacancy, the insertion of two tritium atoms leads to the most energetically favorable defect. The formation of two Fe—T bonds in the vacancy space makes the energy of a doubly tritiated Al vacancy 0.36 eV lower than a non-tritiated Al vacancy. For three tritium atoms inserted in the vacancy space, the defect is isoenergetic with the formation of a non-tritiated Al vacancy. For one tritium atom inserted in a Fe or Al vacancy, the trapping energy E_{Trap} is -0.06 eV or -0.53 eV respectively. The combined energies of a metal vacancy and an interstitial tritium atom (i.e., $\text{V}_\text{M} + 1\text{T}_i$) is shown in Figure 4b by short lines symbols.

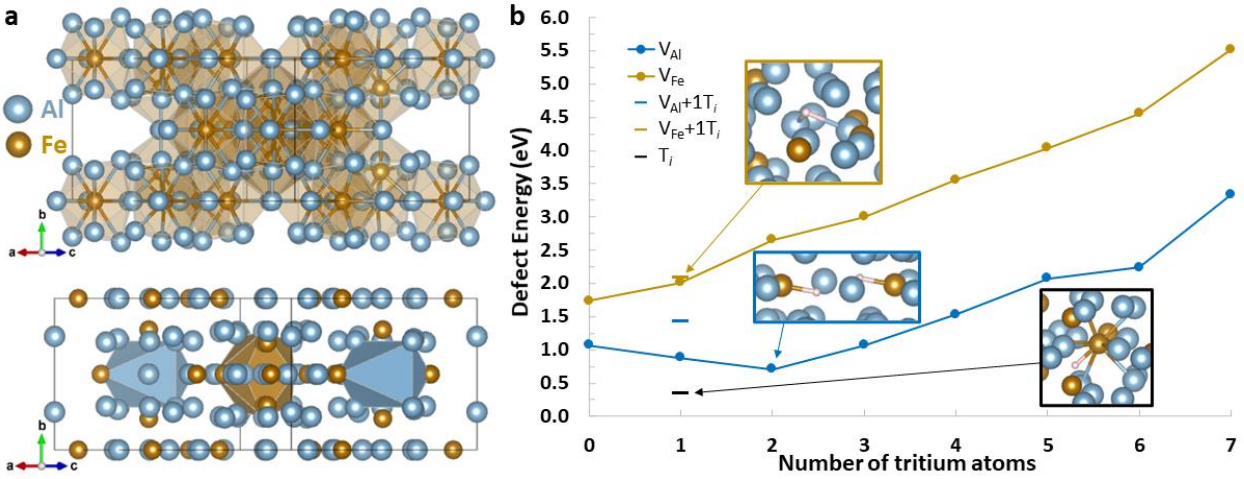

Figure 4: (a) Structural representation of the monoclinic Fe_4Al_{13} phase along with the location of the lowest energy vacancy defects for Fe and Al species as highlighted by a polyhedron. (b) Defect formation energy of metal vacancies as function of tritium loading.

3.3 Tritiation of metal vacancies in the Fe_2Al_x series

The calculations of metal vacancies in the Fe_2Al_x series have been carried out for three stoichiometries, namely Fe_2Al_4, Fe_2Al_5, and Fe_2Al_6. While the ideal stoichiometry of this phase is $Fe_2Al_{5.6}$,[3,10] these specific stoichiometries have been chosen in order to explore the effect of Al vacancy concentration in the channel, going from 100% of Al vacancy, down to 50%, and 0%, as shown in Figure 5a. To identify the Fe and Al sites which are the most favorable for a vacancy, atoms have been removed at different locations. In contrast to the two other Fe-Al phases, Table 2 suggests vacancy generation at each Fe and Al site adjacent to the channel have very similar formation energy for vacancies.

For all three stoichiometries investigated, Figure 5(b-d) suggest that the tritiation of a Fe vacancy is generally not energetically favorable. This trend follows the same behavior that was previously obtained for the other Fe-Al phases. However, the tritiation of an Al vacancy adjacent to the channel is generally found to be energetically favorable, with a maximal energy gain obtained for three, five, and one tritium atoms inserted in the Al vacancy of Fe_2Al_4, Fe_2Al_5, and Fe_2Al_6 respectively. In all these configurations, Fe—T bonds have been formed. While Fe_2Al_4 does not have Al in the channel, the lowest configuration for an interstitial tritium atom is near the center of the channel and bound to two Al atoms adjacent to the channel, as shown in Figure 5b. For Fe_2Al_5, the insertion of tritium atoms in the channel Al vacancy tends to reduce the formation energy of a vacancy. The most favorable tritium loading has been obtained for four tritium atoms inserted in the Al vacancy channel with the formation of four Fe—T bonds. In the case of Fe_2Al_6, the tritiation of an Al vacancy in the channel induces almost no extra energy cost for up to two tritium atoms, then further addition of tritium lead to less energetically favorable formation energies. For one tritium atom inserted in a Fe or Al vacancy of Fe_2Al_4, the trapping energy E_{Trap} is -0.43 eV or -1.43 eV respectively, suggesting that one tritium trapped in a Fe or Al vacancy is energetically preferrable than having a non-interacting metal vacancy and an interstitial tritium atom. The combined energies of a metal vacancy and an interstitial tritium atom (i.e., $V_M + 1T_i$) is shown in Figure 5(b-d) by short lines symbols. For Fe_2Al_5, the trapping energies of a single tritium atom are -0.66 eV, -1.13 eV, and -1.39 eV for Fe, Al, and channel Al vacancies respectively.

For Fe_2Al_6, the trapping energies of one tritium atom are -0.34 eV, -1.99 eV, and -0.45 eV for Fe, Al, and channel Al vacancies respectively.

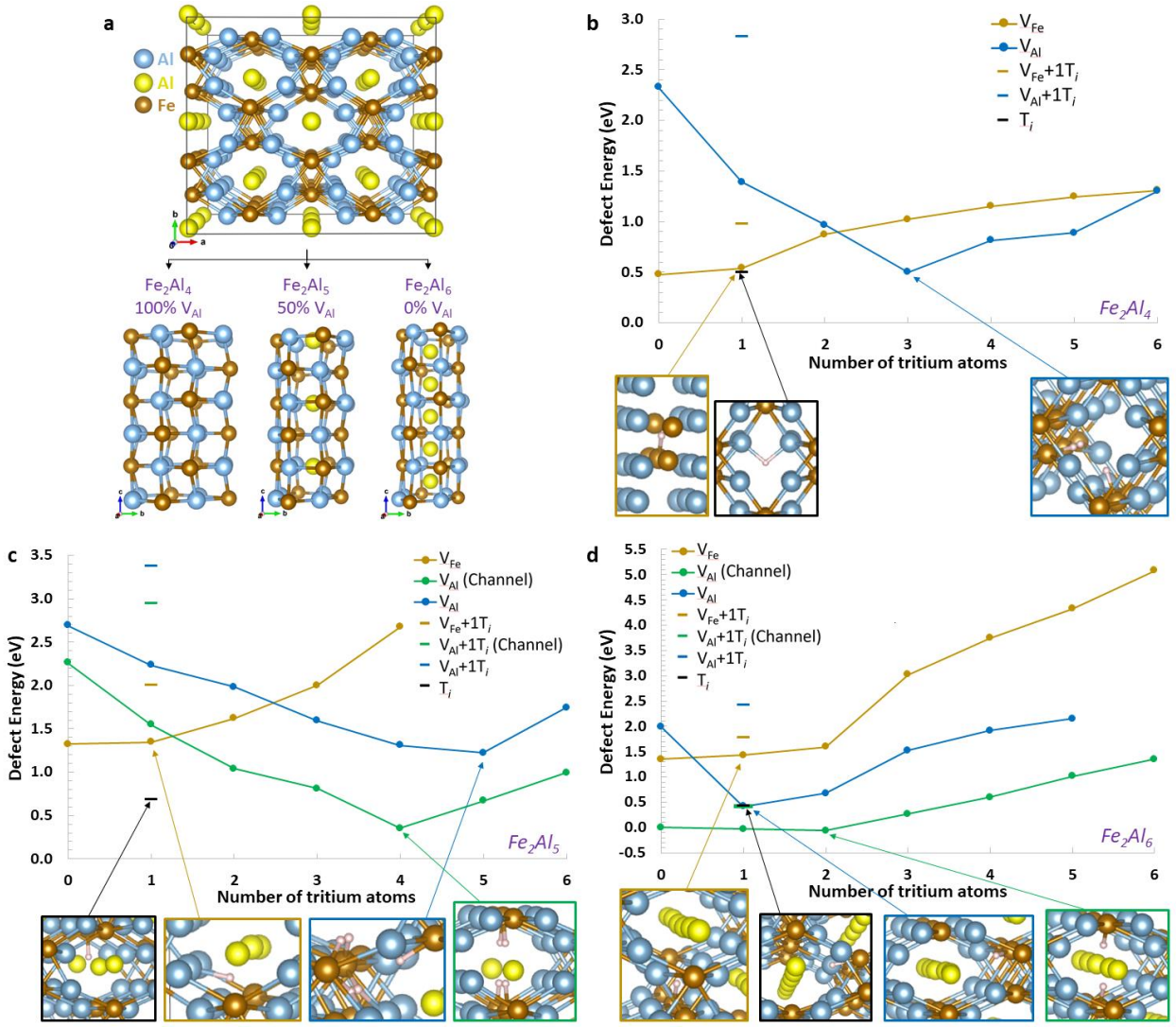

Figure 5: (a) Structural representation of Fe_2Al_x for which the different stoichiometries are associated to the variable presence of Al in the channels as represented by the yellow spheres. (b-d) Defect formation energy of metal vacancies as function of tritium loading for Fe_2Al_4, Fe_2Al_5, and Fe_2Al_6.

Across the Fe-Al phases investigated, the general trends are that Fe and Ni vacancies are not favorable defects for tritium trapping, in contrast to Al vacancies, as shown in Figure 6a. The favorable trapping of tritium atoms in Al vacancies is correlated to the formation of Fe—T bonds. However, it is interesting to note that while tritium is generally not favorably trapped by Fe vacancies, the energy cost for trapping a tritium in a Fe vacancy depends on the Fe-Al phase. As shown in Figure 6a, the trapping of one tritium atom in a Fe vacancy is more favorable in the Fe_2Al_x series, followed by the Fe_4Al_{13} phase, and then by the $FeNiAl_5$ phase. A similar trend

between the Fe-Al phases is obtained for the trapping of one tritium atom in an Al vacancy. Altogether, Figure 6 suggests that the Fe_2Al_x series is the aluminide phase that exhibit the most potential for tritium trapping.

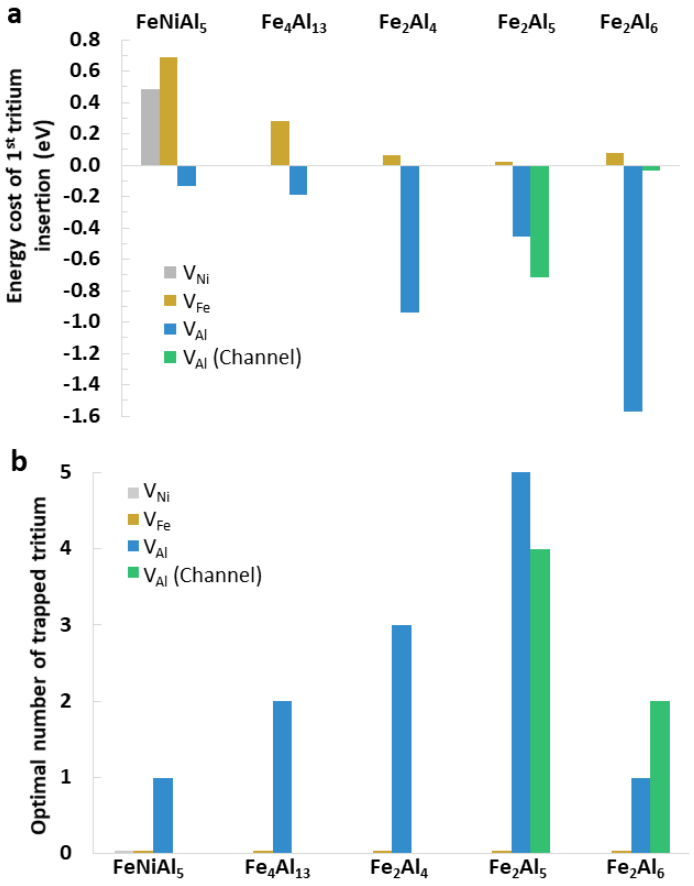

Figure 6: (a) Energy cost calculated for the insertion of the 1st tritium atom in each species site. (b) Summary of the optimal number of tritium inserted in a metal vacancy leading to the lowest defect energy, based on 0 K calculations.

3.4 Effect of temperature and tritium partial pressure

In order to investigate the effect of temperature and tritium partial pressure on the relative thermodynamic stability of tritiated and non-tritiated metal vacancies, *ab initio* thermodynamic calculations have been performed. This allows calculation of the Gibbs free energy of defects at conditions relevant to in-reactor operation at a temperature of 700 K and a range of tritium partial pressures. Figure 7 summarizes the relative thermodynamics for the most energetically favorable defects in each aluminide phase and the purple areas highlight a tritium partial pressure of potential interest.[14] By comparing the energy of tritiated metal vacancies to non-tritiated metal vacancies in each respective Fe-Al phase, a trend can be drawn. At a temperature of 700 K, Figure 7a shows that tritiated vacancies in $FeNiAl_5$ are always higher in energy than non-tritiated metal vacancies over the range of $p(T_2)$ investigated. At $p(T_2)$=1 mbar, the Gibbs free energy difference between a singly tritiated Al vacancy and a non-tritiated Al vacancy, is 0.59 eV. In the

case of Fe_4Al_{13}, Figure 7b shows that tritiated metal vacancies are generally less energetically favorable than non-tritiated metal vacancies over the $p(T_2)$ range of interest, except for a singly tritiated Al vacancy which can compete energetically with non-tritiated Fe vacancies. Interestingly, the energy difference between tritiated and non-tritiated Al vacancies is smaller than for $FeNiAl_5$. Especially, it was found that at $p(T_2)$=10^{-4} mbar a singly tritiated Al vacancy is iso-energetic with a non-tritiated Fe vacancy, indicating that tritiated vacancies can energetically compete with non-tritiated vacancies for high tritium partial pressures. However, a singly tritiated Al vacancy is less energetically favorable than a non-tritiated Al vacancy. In the case of the Fe_2Al_x family, Figures 7(c-e) show that tritiated metal vacancies can compete with non-tritiated vacancies. Over a $p(T_2)$ range of 10^{-6} mbar to 10^2 mbar, a singly tritiated Fe vacancy in Fe_2Al_4 is more thermodynamically stable than a non-tritiated Al or Fe vacancy. In Fe_2Al_5, a singly tritiated Fe vacancy is found more stable than each type of non-tritiated metal vacancy. In the case of Fe_2Al_6, a singly tritiated Al vacancy and doubly tritiated Al channel vacancy are found to be more stable than a non-tritiated Al and Fe vacancy.

The overall analysis of the Gibbs free energy for tritiated and non-tritiated defects at conditions relevant to in-reactor operations follows the trend obtained previously suggesting that the Fe_2Al_x family of materials has more potential for tritium trapping in metal vacancies, followed by Fe_4Al_{13}, then $FeNiAl_5$.

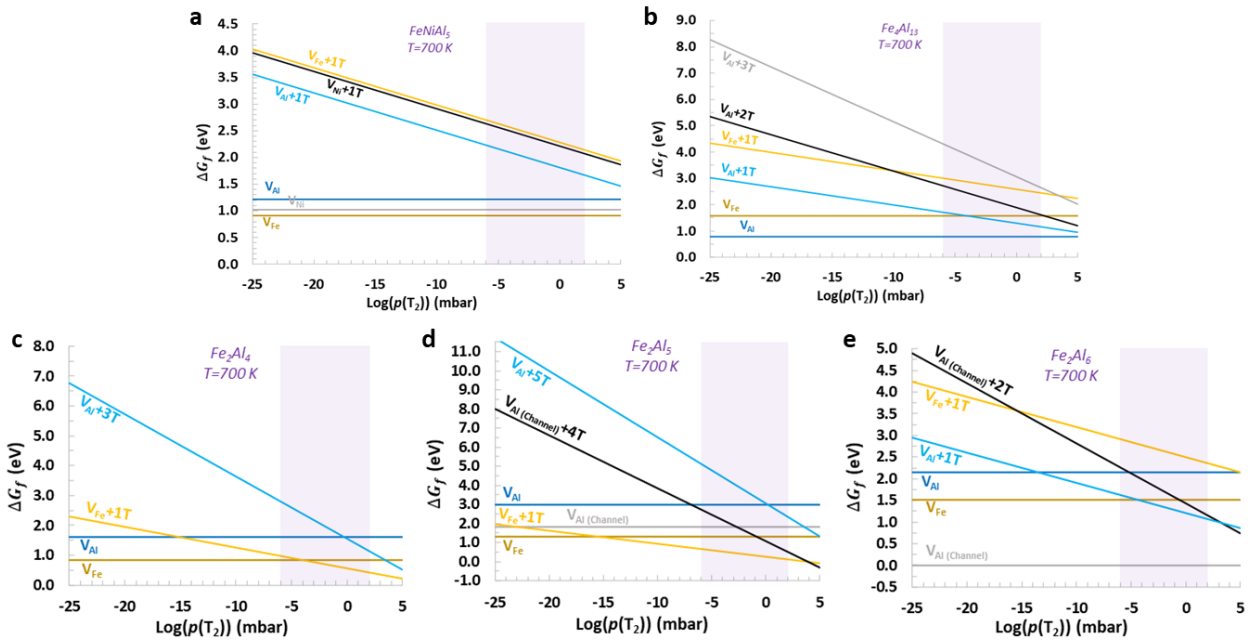

Figure 7: Gibbs free energy of defect formation as function of tritium partial pressure ($p(T_2)$) at a temperature of 700 K for (a) $FeNiAl_5$, (b) Fe_4Al_{13}, (c) Fe_2Al_4, (d) Fe_2Al_5, and (e) Fe_2Al_6. The area in purple highlights the range of tritium partial pressure of interest.

3.5 Interstitial binding energies of Tritium in $FeNiAl_5$, Fe_4Al_{13}, Fe_2Al_4, Fe_2Al_5, and Fe_2Al_6.

Occupation of interstitial sites in defect-free Fe-Al phases is connected to the intrinsic solubility of tritium. Experimentally, solubility is defined as the volume of T_2 gas absorbed by 100 grams of metal. The absorption occurs due to thermodynamics driving gaseous T_2 to dissociate (at the surface or in the metal) and individual T atoms to diffuse and occupy interstitial sites. Solubility is an equilibrium phenomenon that depends on the difference in free energies between a T atom in gas-phase T_2 and in an interstitial site in the Fe-Al phase. Hence solubility can be predicted by Sieverts' Law, which states the solubility of a diatomic gas in a metal is proportional to the square root of the partial pressure of the gas in thermodynamic equilibrium,[15] namely $c_{at} = (Kp(T_2))^{1/2}$ where c_{at} is the concentration of dissolved T atoms, and K is the equilibrium constant for the reaction $T_{2(gas)} \Leftrightarrow 2T_{(dissolved\ in\ metal)}$.

A quick way to screen for relative solubilities under conditions of interest is to determine the interstitial site with the lowest T binding free energy. Note that a full solubility determination requires simultaneous occupation of an ensemble of interstitial binding sites in a metal phase and calculation of their interaction energies as part of the free energy determination. A search for the lowest free energy binding sites was conducted in all the Fe-Al phases examined in this study: $FeNiAl_5$, Fe_4Al_{13}, Fe_2Al_4, Fe_2Al_5, and Fe_2Al_6. The free energy of a single T atom absorbed into an interstitial site in each phase at 700 K as a function of $p(T_2)$ in shown in Figure 8.

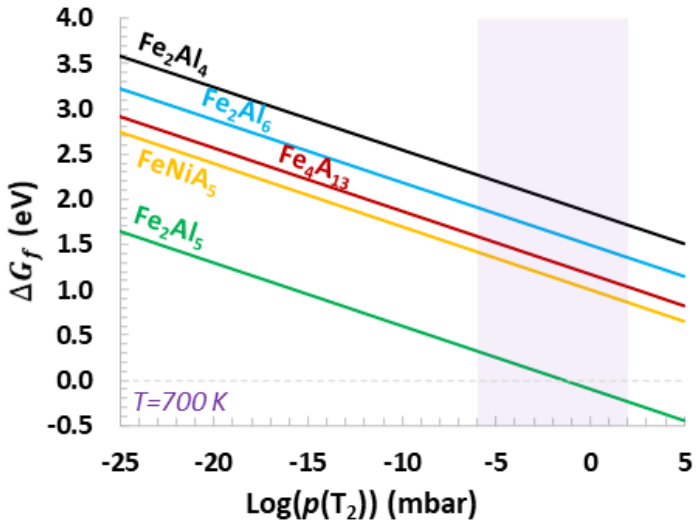

Figure 8: Comparison of the Gibbs free energy for binding an interstitial tritium in the various Fe-Al phases as function of $p(T_2)$ at T=700 K.

In Figure 8, the favorable binding of a single T atom in an interstitial site under reactor conditions would be indicated if the free energy became negative within the purple region (log($p(T_2)$) from -6 to 2). The fact that none of the free energies of binding cross the zero line and become negative except for Fe_2Al_5 in the range of $p(T_2)$ of interest indicates that $p(T_2)$ is generally not sufficient to drive T atoms into the interstitial sites. However, the result that interstitial tritium favorably binds to Fe_2Al_5 and not Fe_2Al_4 or Fe_2Al_6 suggests that the Al occupancy of the channel is an important factor that can affect interstitial tritium behavior in the Fe_2Al_x family of materials.

Conclusion

Density functional theory simulations have been carried out to investigate the potential for tritium trapping by metal vacancies in five different Fe-Al aluminide coating phases. It was found that tritiation of Fe and Ni vacancies is generally less favorable than the tritiation of Al vacancies. However, for the first tritiation, a trend in the defect formation energy can be obtained such that metal defects in the Fe_2Al_x family of materials trap tritium species more favorably than metal vacancies in Fe_4Al_{13} and $FeNiAl_5$. Further investigations using *ab initio* thermodynamics calculations confirmed that trend for a range of tritium partial pressure at a temperature of 700 K. Especially, it was shown that the energy difference between tritiated and non-tritiated metal vacancies is smaller and more favorable for Fe_2Al_x, followed by Fe_4Al_{13}, and $FeNiAl_5$. While this study shows that tritium interacts differently in the various Fe-Al aluminide phases, it also suggests that tritium trapping and retention could be more efficient if metal defects are present in some Fe-Al phases.

Acknowledgments

This research was supported by the National Nuclear Security Administration (NNSA) of the U.S. Department of Energy (DOE) through the Tritium Science Research Supporting the Tritium Modernization Program (TMP) managed by Pacific Northwest National Laboratory (PNNL). The authors thank the PNNL Institutional Computing (PIC) facility for providing computational resources.

4.0 References

1. Burgeson, I.E. *Watts Bar Cycle 12 Rod 2A PIE Protium and Tritium Assay Results.*
2. Edwards, D.J.; Olszta, M.J.; Sunderland, D.J.; Devaraj, A.; Schemer-Kohrn, A.L.; Matthews, B.E. “PIE of cycle 13 316SS cladding using aberration corrected STEM”. Presentation at *Tritium Science Technical Exchange*, Virtual, Washington. PNNL-SA-156394 **(September 2020)**.
3. Sakidja, R.; Perepepzko, J.H., Calhoum, P. “Synthesis, Thermodynamic Stability and Diffusion Mechanism of Al_5Fe_2-Based Coatings”. *Oxid. Met.* **81**, 167-177 (2014).
4. Mihalkovič, M.; Widom, M. “Structure and stability of Al_2Fe and Al_5Fe_2: First-principles total energy and phonon calculations.” *Phys. Rev. B* **85**, 014113 (2012).
5. Sassi, M.; Senor, D.J. “Tritium diffusion in Fe-Al aluminide coating bulk phases”. Presentation at *Tritium Science Technical Exchange*, Virtual, Washington. PNNL-SA-166531 **(September 2021)**.
6. Kresse, G.; Furthmüller, J. “Efficient iterative schemes for ab initio total-energy calculations using a plane-wave basis set”. *Phys. Rev. B* **54**, 11169-11186 (1996).
7. Perdew, J.P.; Burke, K.; Ernzerhof, M. “Generalized Gradient Approximation Made Simple”. *Phys. Rev. Lett.* **77**, 3865-3868 (1996).
8. Eliner, M.; Röhrer, T. “Zur Struktur der ternären Phase $FeNiAl_5$/On the Structure of the Ternary Phase $FeNiAl_5$”. *Int. J. Mater. Res.* **81**, 847-849 (1990).
9. Grin, J.; Burkhardt, U.; Ellner, M.; Peters, K. “Refinement of the Fe_4Al_{13} structure and its relationship to the quasihomological homeotypical structures”. *Z. Kristallogr. Krist.* **209**, 479-487 (1994).
10. Burkhardt, U.; Grin, Y.; Ellner, M. “Structure refinement of the iron-aluminium phase with approximate composition Fe_2Al_5”. *Acta Cryst.* **B50**, 313-316 (1994).
11. Monkhorst, H.J.; Pack, J.D. “Special points for Brillouin-zone integrations”. *Phys. Rev. B* **13**, 5188 (1976).
12. Togo, A. and Tanaka, I. “First principles phonon calculations in materials science”. *Scr. Mater.* **108**, 1-5 (2015).
13. *NIST-JANAF Thermochemical Tables*, 4th Edition, edited by J.M.W. Chase American Chemical Society, Washington, DC, **1998**.
14. Luscher, W.G; Senor, D.J.; Clayton, K.K.; Longhurst, G.R. “In situ measurement of tritium permeation through stainless steel”. *J. Nucl. Mater.* **437**, 3730379 (2013).
15. Gupta, C.K. “Chemical metallurgy: principles and practice”, Wiley-VCH, **2003**, p. 273.

Pacific Northwest National Laboratory

902 Battelle Boulevard
P.O. Box 999
Richland, WA 99354
1-888-375-PNNL (7665)

www.pnnl.gov